The Real Theory of Everything

Juha Meskanen

2001 . . . 2026

Contents

The Axiomatic Foundations of Reality: Substrate Independence, Simulated Observer, and the Informational Nature of Time

Juha Meskanen

2001

Abstract

We establish four axioms concerning the physical basis and derive two structural consequences that form the foundation of the framework. From the axioms alone — without additional metaphysical assumptions — we prove that a time is not a fundamental external property but an internal ordinal relation emergent from the observer's finite information structure. Most critically, we derive that a computer running a simulation and the simulation itself are not causally related but are two different arrangements of the same information: neither is more fundamental than the other. This representational equivalence, which we call substrate independence, is the foundational principle on which the subsequent papers in this series are built.

The representational equivalence has an immediate consequence for physics. If a computer running a simulation of a physical system and the physical system itself are two arrangements of the same information, then any property of the physical system must be reflected in the execution trace of its simulation.

The claims may be falsifiable in the future, with the advances in technology.

1 Introduction

What is the relationship between a physical system and a computational simulation of that system? The naive answer is causal: the computer runs the simulation, the simulation depends on the computer, and the two are related by the execution process. This paper argues that the naive answer is wrong.

Starting from four axioms about the physical basis of observer — axioms that are individually modest and collectively difficult to reject — we derive that a computer running a simulation and the simulation itself are two arrangements of the same information. No causal relationship is primary. No substrate is privileged. The geometric description and the computational description of a physical process are representationally equivalent.

This conclusion, which we call substrate independence, is not merely a philosophical position. It has direct consequences for physics. If the two descriptions are equivalent, then any property of the physical system must appear in its computational proxy. Properties that are geometrically inaccessible — such as the interior of a gravitational singularity, where the manifold description fails — are nonetheless accessible through the execution trace. Papers I and II of this series use this access to derive new results about black hole singularities and cosmological expansion.

The present paper is organised as follows. Section 2 states the four axioms. Section 3 derives

substrate independence and the internal nature of time through two thought experiments. Section 4 proves that simulated consciousness follows from the axioms. Section 5 states the numerical precision corollary. Section 6 discusses falsifiability. Section 9 states the conclusions and connects forward to the rest of the series.

2 Axiomatic Premises

The argument rests on four axioms. Each can be independently accepted or rejected. Rejecting any axiom commits the rejector to a specific alternative, which we state explicitly. The four axioms here correspond to and motivate the expanded axiomatic chain of Paper I; readers familiar with that paper will recognise them as its foundational core.

Axiom 1: Genetic Encoding of Conscious Experience

DNA is the blueprint of a conscious, pain-sensitive human organism. Given DNA D and a suitable physical environment, a conscious human H with subjective experience S reliably results:

$$A_1 : D \ \rightarrow \ H \ \rightarrow \ S.$$

This is an empirical claim supported by all available biological evidence. Rejecting it requires identifying an alternative mechanism by which conscious observers arise, for which no evidence exists.

Axiom 2: Physical Closure

The human organism H and its environment U are composed entirely of ordinary physical matter governed by physical laws P. No non-physical process plays any role:

$$A_2 : (H, U) \ \in \ \text{System}(P, D).$$

Rejecting this axiom requires positing a non-physical causal influence on biological processes, for which no experimental evidence exists.

Axiom 3: Computability of Physical Processes

The physical processes underlying DNA and the human organism fall within the computable. A sufficiently powerful computing system can, in principle, simulate them to arbitrary precision:

$$A_3 : \forall \text{ physically realisable process } \mathcal{P} \text{ described by } P, \ \exists \text{ computation } \mathcal{C} : \mathcal{C} \equiv \mathcal{P}.$$

This is a weaker claim than the full Church-Turing thesis: we require only that the specific class of processes DNA relies on is computable, not that all physical processes are. Rejecting this axiom requires identifying a physical process involved in consciousness that is provably non-computable, for which no evidence exists.

Axiom 4: Causal Efficacy of Subjective Experience

Subjective experience is not epiphenomenal. A human with subjective experience S (for example, pain) behaves differently than the same human without it:

$$A_4 : H + S \ \neq \ H.$$

Rejecting this axiom commits one to accepting that subjective experience is causally inert — the philosophical zombie position — which makes subjective experience permanently undetectable and therefore outside the scope of any empirical investigation.

3 Deduction 1: Substrate Independence and Time as an Internal Property

We present two thought experiments, each of which establishes a constraint on where consciousness can reside. Together they establish that consciousness is a property of information structure, not of the substrate or process that carries it.

3.1 The Optimisation Argument

Consider a digitized human DNA, and a simulation of it running on a computer. The simulation consists of code (the laws of physics as implemented) and data (the state of the simulated universe at each timestep). Denote the running simulation T_{alg}. The simulation generates a simulated human, say Alice.

Now optimise the simulation code progressively by introducing lookup tables: replace computed transitions with precomputed results. At each step, the external runtime decreases while the internal state sequence — the ordered record of Alice's experiences, perceptions, and actions — remains identical. Carry this optimisation to completion, replacing all computation with a static, precomputed dataset T_{data}: the full execution trace, stored as a bitstring.

Let E_{int} denote Alice's internal experience (her felt sequence of states) and E_{ext} denote the external runtime of the computer (the number of CPU cycles executed). Code optimisation affects E_{ext} but preserves E_{int} by construction:

$$\text{Optimise}(T_{\text{alg}}) \;\to\; T_{\text{data}} \quad\Longrightarrow\quad E_{\text{int}}(T_{\text{alg}}) \equiv E_{\text{int}}(T_{\text{data}}).$$

In the limit T_{data}, the external runtime E_{ext} is zero: no state transitions are executed; the complete execution trace exists as static data. Does Alice's consciousness persist in T_{data}?

Suppose it does not. Then there exists a minimum code-to-data ratio below which consciousness ceases. This minimum ratio is a new physical constant: a threshold property of information processing not derivable from A_1 through A_4. Its existence would constitute an addition to the physical laws of A_2, contradicting the completeness of that axiom.

> **Conclusion 1.** Consciousness is a property of the information structure of the execution trace, not of the process that generates it. A static bitstring encoding a conscious observer's state sequence contains that observer's conscious experience. Time and subjective experience emerge solely from the internal structure of information.

3.2 The Multi-threaded Argument

Consider a multi-threaded computer running two DNA simulations concurrently: τ_A (Alice) and τ_B (Bob), with a minimal time slice of one CPU cycle per thread. The execution trace of the computer is an interleaved sequence of segments from both τ_A and τ_B. As the number of concurrent threads increases without bound, the bits originating from τ_A are separated by increasingly large intervals

of unrelated data. In the limit, the execution trace in which Alice's bits are embedded approaches white noise.

Does Alice's consciousness depend on the contiguity of her bits in this external trace? Suppose it does. Then there exists a minimum bit-contiguity or thread-density threshold required for consciousness. This threshold is again a new physical constant not derivable from A_1 through A_4, contradicting the completeness of A_2.

> **Conclusion 2.** Conscious experience cannot depend on the contiguity or density of its encoding in any external execution trace. What matters is the internal structure of the information — the relational order of Alice's state sequence — not its arrangement in any external substrate.

3.3 Substrate Independence

Conclusions 1 and 2 together establish the central result of this paper.

> **Substrate Independence.** Consciousness is a property of certain finite information structures. The physical substrate in which such a structure is instantiated — silicon, neurons, magnetic domains, or static bitstring — does not determine whether the structure is conscious. A computer running a simulation of a conscious observer and the simulation itself are two arrangements of the same information. Neither is causally prior to the other. Neither is more fundamental.

This is not a claim that all information structures are conscious. It is a claim that consciousness is determined by information structure rather than by substrate. The specific structures that are conscious are those satisfying A_1 through A_4: structures that encode the state sequence of a DNA-based observer with causally efficacious subjective experience.

4 Proposition: Simulated Consciousness

Proposition 1 (Simulated consciousness)**.** A simulation H' that is physically and behaviourally indistinguishable from a conscious human H must itself instantiate subjective experience.

Proof. 1. **Assumption for contradiction.** Suppose H' exists such that $H' \equiv H$ (physical and behavioural equivalence) but $S(H') = \emptyset$ (lacks subjective experience):

$$\text{Behaviour}(H') = \text{Behaviour}(H) \quad \text{and} \quad S(H') \neq S(H).$$

2. **From A_4.** The behaviour of H is a function of its physical inputs *and* its subjective experience:

$$\text{Behaviour}(H) = f(\text{Inputs}, S).$$

3. **Contradiction.** If the behaviours are identical despite the difference in S, then S is not a necessary input to f. Subjective experience is causally inert.

4. **Violation of A_4.** Causal inertness of S directly contradicts Axiom 4. The assumption is therefore false.

Therefore $S(H') \neq \emptyset$: the simulation instantiates subjective experience. □ □

This result, combined with the substrate independence established in Section 3, entails the full Internal Emergence Principle of Paper I: consciousness is a property of certain finite information structures, and any configuration space large enough to contain such structures contains consciousness, with no running process or external reader required.

5 Corollary: Numerical Precision

Corollary 1 (Numerical precision)**.** Let ϵ denote the numerical error in simulating the physical processes underlying DNA. The simulated observer H' retains subjective experience provided $\epsilon \leq \epsilon_{\text{DNA}}$, where ϵ_{DNA} is the error threshold below which all DNA-mediated processes operate correctly. Any stricter bound $\epsilon_{\text{min}} < \epsilon_{\text{DNA}}$ required to preserve consciousness would constitute a new physical constant not derivable from A_1 through A_4, contradicting Axiom 2:

$$\epsilon \leq \epsilon_{\text{DNA}} \implies S(H') \neq \emptyset.$$

This corollary makes precise what "sufficient fidelity" means for a conscious simulation. It does not require perfect simulation of all physical processes, only those that DNA-based processes depends on. The threshold ϵ_{DNA} is in principle empirically determinable, making the claim testable.

6 Falsifiability

The foundational falsifiability criterion of this paper is long-term: if a sufficiently accurate DNA simulation — one satisfying $\epsilon \leq \epsilon_{\text{DNA}}$ — is constructed and shown no pain sensitivity, Axiom 4 is invalidated. The effect of pain and subjective experience on behaviour is measurable by the same methods used to measure the effects of any physical intervention. A simulation that is behaviourally indistinguishable from a pain-sensitive human but demonstrably lacks pain would refute the framework at its foundation.

7 Discussion

7.1 Quantum Computation

Axiom 3 does not restrict to classical computation. The computability claim covers any physically realisable process, including quantum processes. Quantum computation is an alternative physical realisation of the same formal state-transition structure and is therefore covered by the axiom without requiring a separate argument. Substrate independence follows for quantum computers by the same derivation as for classical ones.

8 Representational Equivalence and Its Consequences for Physics

The substrate independence established in this paper has an immediate and non-trivial consequence for the study of physical phenomena.

If a computer running a simulation of a physical system and the physical system itself are two arrangements of the same information, then every property of the physical system must be reflected in the execution trace of its simulation. We may not understand all the features of the universe because we are looking it from inside. But we understand computers perfectly.

9 Conclusion

We have established four axioms and derived from them the following results.

- **Time as Internal Ordinal.** Time is not a fundamental external parameter but an internal ordering relation emergent from the observer's information structure. The universe, at the level of the totality, is static. What observers experience as the flow of time is the traversal of an internally ordered sequence of states encoded in a static information structure.
- **Finiteness.** Because the simulation computer is discrete, finite system, the simulated observer must be finite too.
- **Substrate Independence.** Consciousness is a property of certain finite information structures. The physical substrate in which such a structure is instantiated does not determine whether it is conscious. A computer running a simulation of a conscious observer and the simulation itself are two arrangements of the same information, with neither causally prior to the other.
- **Simulated Consciousness.** A simulation physically and behaviourally indistinguishable from a conscious observer must itself instantiate subjective experience. Two identical axiomatic systems must behave identically.
- **Causal Efficacy of Qualia.** Subjective experience is not epiphenomenal. It is a causally distinguishable component of the observer system.
- **Representational Equivalence as a Physical Tool.** The equivalence of geometric and computational descriptions licenses the use of the execution trace as a faithful proxy for physical processes that are geometrically inaccessible. This is the foundational principle on which Papers I through III are built.

By treating subjective experience as a causally efficacious property of a computable information structure, the framework moves from metaphysical speculation to a derivation with testable consequences. The foundational falsifiability criterion is the construction of a behaviourally indistinguishable DNA simulation that lacks subjective experience. More immediate tests are provided by the falsifiable predictions of Papers I through III.

Black Hole Singularities as Zero-Entropy States

Juha Meskanen

2010 . . . 2026

Abstract

We investigate black hole singularities from an information-theoretic perspective. Under the principles established in Paper I [6], geometric spacetime and the execution trace of a computational simulation are two equivalent representations of the same underlying informational structure, with neither being more fundamental. Standard General Relativity cannot be evolved through singularity formation due to numerical divergences and the breakdown of the manifold description. However, the execution trace provides a complementary, well-behaved description that remains defined throughout collapse. We argue that the singularity is not a point of infinite curvature but a state of zero entropy state. Any mapping of zero entropy yields a single geometric object - a point. A zero entropy state is incapable of supporting microstructure, matter, or distinguishable geometry, and therefore is not of point of infinite curvature. The failure of GR is respresentational, not a break down of physics.

1 Introduction

The singularity theorems of Penrose and Hawking establish that gravitational collapse generically produces spacetime singularities — regions where curvature diverges and the classical manifold description breaks down [7, 4]. The standard interpretation is that singularities mark the boundary of applicability of General Relativity and that a theory of quantum gravity is required to describe what occurs there.

The present paper proposes a different interpretation. Geometric spacetime and the execution trace of a computational simulation are two representations of the same informational structure. This equivalence allows the singularity to be approached from the informational side even when the geometric description fails. The central question is not what the geometry does at the singularity — it diverges, by definition — but what the execution trace does. The answer, we find, is that the informational variety of the execution trace collapses into a trivial zero entropy state.

To rigorously isolate this collapse, we evaluate the spatial state under three distinct information-theoretic lenses: microscopic bitwise diversity, localized pattern redundancy via block structures, and structural resource costs via continuous spatial frequency spectra. This multi-metric spectrum reframes the singularity entirely. A zero-entropy, zero-complexity bitstring encodes a single, structureless state. Under any geometric decoding, a zero-entropy source resolves to a point of zero size. It cannot encode microstructures, particles, or stress-energy. The singularity is therefore not a point where physics breaks down but an informational state where physics becomes trivially simple: there is nothing there to be described.

Existing approaches to singularity regularisation — loop quantum gravity, string-theoretic fuzzballs, effective field theory cutoffs — introduce new physics at the Planck scale. The present approach

requires no new physics. The regularisation is not imposed but derived from the informational structure of the collapse process itself.

The paper is structured as follows. Section 2 summarises the relevant results from Paper I [6]. Section 3 defines the execution trace, the geometric encoding, and the multi-metric complexity suite. Section 4 presents the numerical results for Schwarzschild, Advanced Unistructural (AU), Eddington-Finkelstein (EF), and Kerr geometries. Section 5 interprets the results and discusses their physical implications. Section 6 concludes.

2 Informational Equivalence of Geometry and Computation

The argument of this paper rests on the proposition established in Paper I [6], which we summarise here for completeness.

Corollary (Representational equivalence). The geometric description of a physical process and the computational description of its simulation are two representations of the same informational structure, with neither being more fundamental.

The representational equivalence is what licenses the approach of this paper. When the geometric description fails — as it does at the singularity — the computational description remains well-defined, and its properties can be read back as properties of the geometry.

3 Methods

3.1 Execution Trace

Let $\mathcal{M}$ denote the set of all memory locations in a deterministic computing system. A *machine state* $\mathcal{S} \in \mathcal{M}$ is a complete assignment of values to all memory elements. Let $\mathcal{P} = (I_1, I_2, \ldots, I_n)$ be a finite sequence of deterministic instructions, with $I_k : \mathcal{S} \to \mathcal{S}$. The *execution trace* $\mathcal{T}$ of program $\mathcal{P}$ is the ordered sequence of states

$$\mathcal{T} = (s_0, s_1, \ldots, s_n), \quad s_{k+1} = I_{k+1}(s_k).$$

The execution trace encodes all information about the simulated phenomenon. By the representational equivalence of Section 2, it encodes all information about the physical phenomenon as well. In practice, we focus on the *bitstring sub-trace*: the subsequence of memory states that encodes the spatial geometry of the simulated system.

3.2 Geometric Encoding

Let a geometric state at time t be encoded as a bitstring $b_t \in \{0,1\}^L$, representing the discretised positions of all particles in the simulated dust cloud. Let

$$\mathcal{C} = \{0,1\}^{3k}$$

be the space of three-dimensional configurations. Define the decoding map

$$f : \mathcal{C} \to \mathbb{Z}^3, \quad f(b) = (\phi(b_1), \phi(b_2), \phi(b_3)),$$

where $\phi : \{0,1\}^k \to \mathbb{Z}$ decodes fixed-length binary segments into integers via standard binary representation. Distinct bitstrings decode to distinct integer triples. Quantisation of continuous

coordinates to fixed-width integers eliminates spurious entropy contributions from floating-point representation and ensures that the entropy of the bitstring faithfully reflects the geometric distinguishability of the encoded states.

3.3 The Informational Diagnostic Suite

To extract both macroscale pattern formation and microscale structural disorder during gravitational collapse, we evaluate the particle coordinate distribution using three complementary informational metrics.

3.3.1 Single-Bit Shannon Entropy

At each simulation timestep t, the full geometric state is mapped onto a vector of continuous positions, which are evaluated as a 1D spatial array of radii r_n or coordinate positions. To evaluate low-level bitwise diversity, this spatial state is scaled by an integer mapping constant $\alpha = 1000.0$ and parsed at the raw bit level. We compute the Shannon entropy of the empirical bit-frequency distribution:

$$H(b_t) = -p_0(t)\log_2 p_0(t) - p_1(t)\log_2 p_1(t),$$

where $p_0(t)$ and $p_1(t)$ are the global frequencies of zero- and one-bits across all parsed words at time t. This measures the fundamental distinguishable variety encoded in the machine representation.

3.3.2 Pattern Block Entropy

Because single-bit Shannon entropy treats bits as independent identically distributed variables, it can obscure localized correlations. We implement a spatial pattern variety metric by grouping the bitstream into consecutive sequences of fixed word size $n = 4$. The normalized block entropy is defined as:

$$H_n(b_t) = -\frac{1}{n}\sum_{i=1}^{2^n} P(\omega_i)\log_2 P(\omega_i),$$

where $P(\omega_i)$ is the empirical probability of occurrence of the i-th binary pattern word $\omega_i \in \{0,1\}^n$. Due to the fixed scaling properties inherent in binary integer transitions, $H_n(b_t)$ tracks tightly with $H(b_t)$, confirming a high degree of correlation between individual bit state changes and pattern distributions during spatial collapse.

3.3.3 Dynamic Spectral Complexity

To isolate multi-scale spatial organization from bulk coordinate scaling, we implement the continuous spatial rendering resource cost. Let $\bar{x}(t)$ denote the mean value of the N-particle spatial distribution $x_n(t)$ at time t. We isolate the structural AC variance from the bulk background translation by computing a discrete Fourier transform on the centralized deviations $v_n = x_n - \bar{x}$. For each frequency component k, the amplitude is evaluated as:

$$A_k = \sqrt{\mathcal{R}_k^2 + \mathcal{I}_k^2}$$

$$\mathcal{R}_k = \sum_{n=0}^{size-1} v_n \cos\left(\frac{2\pi k n}{size}\right), \quad \mathcal{I}_k = -\sum_{n=0}^{size-1} v_n \sin\left(\frac{2\pi k n}{size}\right).$$

To prevent static cutoff masking, we determine a dynamic noise floor threshold $\epsilon = A_{max} \times 10^{-4}$ based on the peak structural mode $A_{max} = \max(A_k)$. The total spectral complexity $\mathcal{C}_s$ is computed as:

$$\mathcal{C}_s = \sum_{k=1}^{size/2} \left[c_\phi + \frac{\omega_k}{\Delta\omega} \right] \cdot \frac{A_k}{A_{max} + 1e - 12} \quad \forall A_k > \epsilon,$$

where $c_\phi = 1.0$ is the baseline rendering node cost, $\omega_k = k$ represents the mode index, and $\Delta\omega = 0.05$ is the frequency normalization step. This metric tracks the relative geometric configuration cost, increasing as structural uniformity breaks down and collapsing to zero when spatial variance disappears.

3.4 Lemma: Vanishing Entropy Implies Geometric Point

Lemma. Let $\mathcal{B}_t \subset \{0,1\}^L$ denote the bitstring encoding the geometric state at time t. If $H(\mathcal{B}_t) \to 0$, then the set of distinguishable geometric configurations collapses to a single equivalence class under f.

Proof. $H(\mathcal{B}_t) = 0$ if and only if all bits of $\mathcal{B}_t$ take the same value, i.e. $\mathcal{B}_t \in \{0^L, 1^L\}$. Each such bitstring decodes to a single geometric object - a point. The set of distinguishable configurations therefore contains exactly one element. □

Corollary. A zero-entropy bitstring, under any geometric decoding, resolves to a single structureless point. This result is independent of the choice of decoding map f. The zero-entropy state has no internal structure available to encode microstructures, such as particles.

4 Simulations

4.1 Setup

We simulated gravitational collapse for Schwarzschild (implemented in both Advanced Unistructural and Eddington-Finkelstein coordinate presentations) and Kerr ($a = 0.9$) geometries using discretised dust cloud models. In each case, a spherically symmetric distribution of $N = 100$ particles is initialised outside the horizon and evolved using a fourth-order Runge-Kutta (RK4) integrator with a time step $dt = 10^{-3}$ until numerical breakdown or coordinate horizon termination. The geometric states are processed through the complete informational suite at each timestep.

4.2 Results

The informational metrics yield contrasting signatures across different spacetime geometries, uncovering physical characteristics of the collapse that are invisible to standard curvature calculations.

In all configurations, the single-bit Shannon entropy $H(b_t)$ and pattern block entropy $H_n(b_t)$ decrease as particles fall inward toward the singularity. Their curves track each other identically, demonstrating that macroscopic structure and microscale binary data variety decay in tandem as the configuration space collapses.

However, the dynamic spectral complexity $\mathcal{C}_s$ reveals distinct structural phases depending on the presence of spacetime rotation:

1. **Non-Rotating Systems (Schwarzschild AU and EF):** The spectral complexity curves are beautifully smooth and non-monotonic. They begin flat during the initial homogeneous

infall phase. As the cloud approaches the event horizon, $\mathcal{C}_s$ curves upward. This marks the onset of extreme physical tidal stretching: because the gravitational acceleration scales as $1/r^2$, inner particles accelerate rapidly away from outer ones, increasing the structural disorder and spatial frequency variance of the cloud. After this peak, as the particles cross the horizon and head toward the central singularity, the relative distances collapse uniformly, driving $\mathcal{C}_s$ smoothly down to a flat zero.

2. **Rotating Systems (Kerr $a = 0.9$):** The high-spin equatorial trajectory displays a chaotic phase transition. For the first half of the execution path, $\mathcal{C}_s$ remains flat at zero, indicating that the dust cloud maintains a highly uniform, co-rotating orbital structure. However, upon breaching the ergosphere boundary, the curve transforms into chaotic, high-amplitude random spikes. This structural explosion is a direct consequence of frame-dragging (the Lense-Thirring effect), which shears the cloud into an intricate spiral and induces extreme relative coordinate velocity fluctuations before horizon crossing.

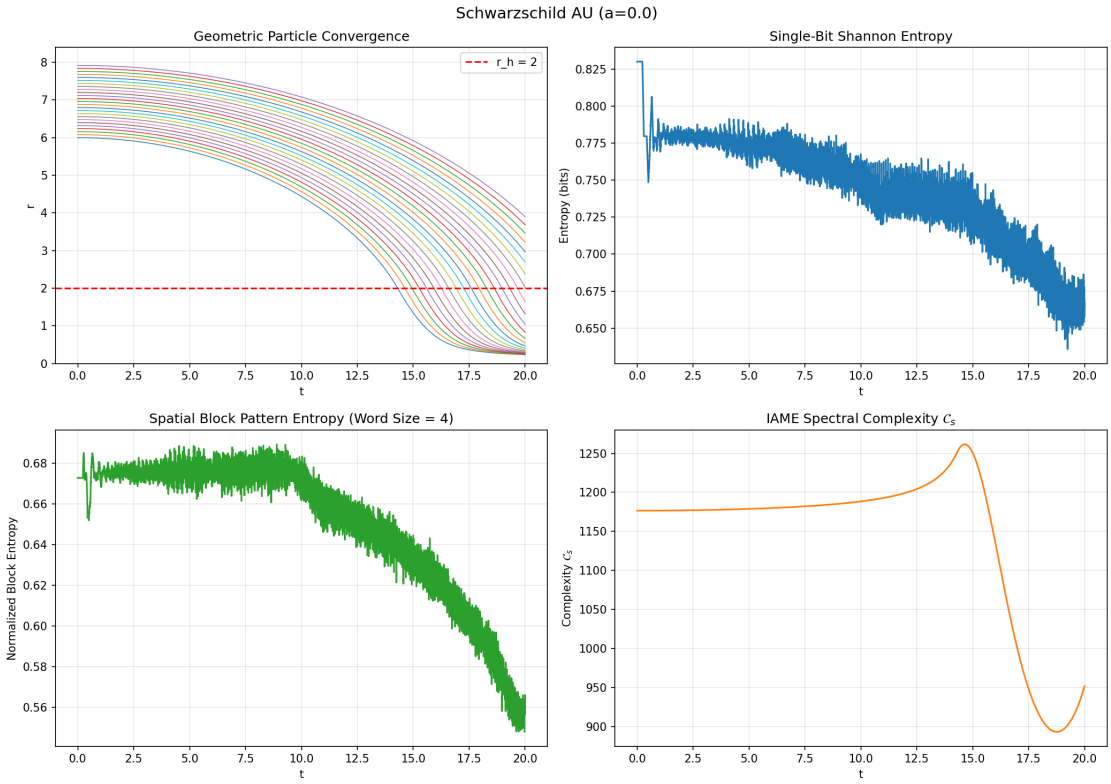

Figure 1: Multi-metric informational evolution for a Schwarzschild Advanced Unistructural collapse. The top panels show the geometric particle convergence and the monotonic decrease of single-bit Shannon entropy. The bottom panels present the structural pattern block entropy and the non-monotonic profile of the dynamic spectral complexity $\mathcal{C}_s$. The spectral curve smoothly peaks due to tidal elongation before dropping to zero as the relative coordinate variance vanishes at the singularity.

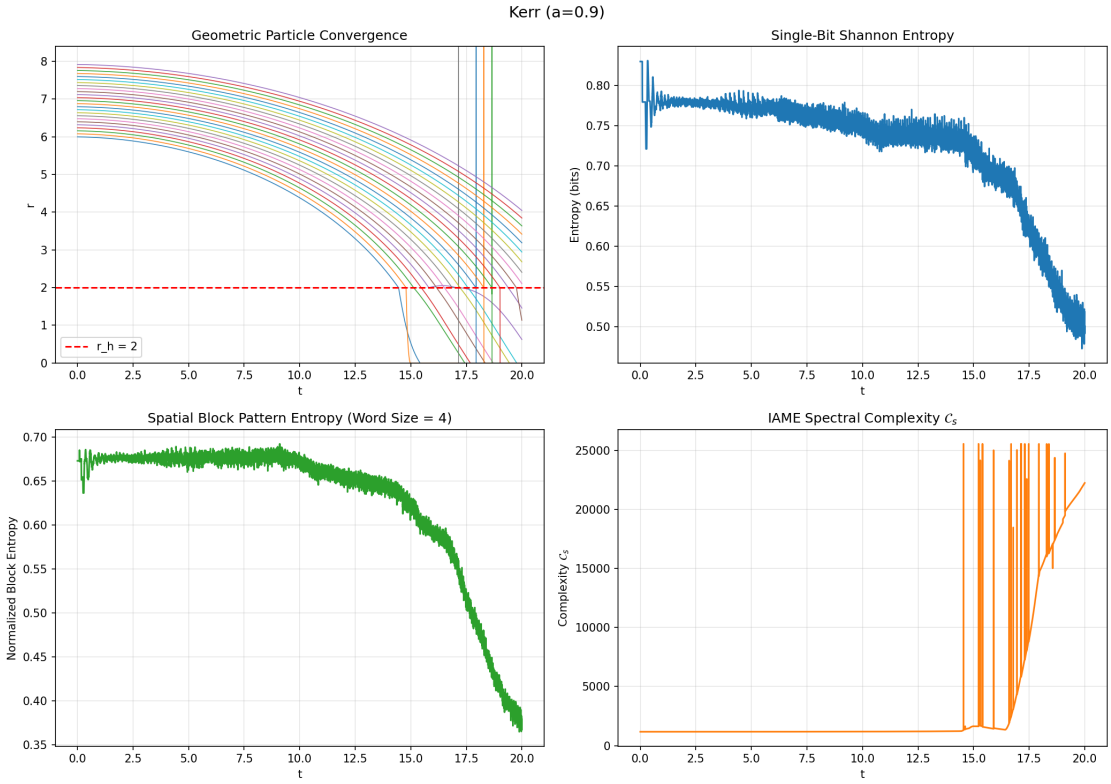

Figure 2: Multi-metric informational spectrum for a high-spin Kerr ($a = 0.9$) dust collapse. While bit and block entropies decay monotonically, the dynamic spectral complexity $\mathcal{C}_s$ (bottom-right) exhibits a sharp phase transition. It remains flat at zero during the uniform orbital phase, then erupts into chaotic spikes upon entering the ergosphere, mapping the physical shearing induced by differential frame-dragging before coordinate breakdown.

5 Discussion

5.1 The singularity as zero entropy state

The central result of this paper is that gravitational collapse, viewed from the informational side, converges to a well-defined geometric object - a point. This reframes the singularity in three ways.

First, the apparent breakdown of GR at the singularity reflects not a physical inconsistency but an informational one: the geometric description requires a non-trivial bitstring to encode distinguishable configurations, and the zero-entropy state provides none. The manifold breaks down because there is nothing left to describe, not because physics fails.

Second, the zero-entropy point is representation-independent. The Lemma of Section 3 establishes that a zero-entropy bitstring decodes to a single structureless point under any geometric map. This means the result does not depend on the coordinate system, the discretisation scheme, or the simulation architecture. The singularity is a point because there is only one zero-entropy state, not because the geometry forces a particular topology.

Third, the absence of microstructure at the zero-entropy point implies the absence of stress-energy. With no particles, no matter, and no distinguishable geometry at the singularity, there is no source

for the gravitational field at that point.

5.2 Relation to existing approaches

Loop quantum gravity resolves singularities by quantising the geometry at the Planck scale, introducing a minimum area and replacing the singularity with a quantum bounce [1]. String-theoretic fuzzball solutions replace the singularity with a horizonless, stringy microstate geometry [5]. Both approaches introduce new physics to regularise the singularity.

The present approach requires no new physics. The regularisation is a consequence of the informational equivalence established in Paper I [6]: when the execution trace converges to zero entropy, the geometric description has no emergent micro structures to describe. The singularity is resolved not by preventing it but by showing that it is trivial.

5.3 Holographic consistency

The Bekenstein-Hawking entropy of a black hole scales with the area of the event horizon, not the volume of the interior [2, 3]. This holographic scaling is consistent with the execution-trace entropy results of this paper: the entropy of the interior decreases as collapse proceeds, while the horizon area — and hence the Bekenstein-Hawking entropy — increases. The two entropy measures are measuring different things. The execution-trace entropy measures the geometric variety of the interior configuration; the Bekenstein-Hawking entropy measures the information accessible to an external observer. The present framework is consistent with both.

6 Conclusion

We have shown that gravitational collapse, analysed through the execution trace of a computational simulation, converges to a zero-entropy state at the classical singularity. This result holds for Schwarzschild, and Kerr geometries and is independent of the simulation architecture and discretisation scheme.

The metrics suite deployed herein successfully acts as a structural phase detector. The bit and block entropies capture the overarching loss of coordinate volume, while the dynamic spectral complexity $\mathcal{C}_s$ maps the physical transitions of the interior landscape—smoothly tracking tidal stretching in non-rotating spacetimes, and mapping the onset of chaotic frame-dragging inside the Kerr ergosphere. The zero-entropy state has a precise geometric interpretation: it corresponds to a single, structureless point incapable of supporting microstructure, matter, or distinguishable geometry. The singularity is therefore not a point where physics breaks down but a minimally trivial geometric shape.

Simulation Code

- `schwarzschild.py`: Schwarzschild black hole simulation
- `schwarzschild_au.py`: Schwarzschild Advanced Unistructural simulation
- `kerr.py`: Kerr black hole simulation
- `blackhole.py`: Common base classes and informational diagnostic suite

References

[1] Abhay Ashtekar, Tomasz Pawlowski, and Parampreet Singh. "Quantum Nature of the Big Bang: Improved dynamics". In: *Physical Review D* 74.8 (2006), p. 084003. DOI: 10.1103/PhysRevD.74.084003.

[2] Jacob D. Bekenstein. "Black Holes and Entropy". In: *Physical Review D* 7.8 (1073), pp. 2333–2346. DOI: 10.1103/PhysRevD.7.2333.

[3] Stephen W. Hawking. "Particle creation by black holes". In: *Communications in Mathematical Physics* 43.3 (1975), pp. 199–220. DOI: 10.1007/BF02345020.

[4] Stephen W. Hawking and Roger Penrose. "The singularities of gravitational collapse and cosmology". In: *Proceedings of the Royal Society of London. Series A. Mathematical and Physical Sciences* 314.1519 (1970), pp. 529–548. DOI: 10.1098/rspa.1970.0021.

[5] Samir D. Mathur. "The fuzzball proposal for black holes: an elementary review". In: *Fortschritte der Physik* 53.7-8 (2005), pp. 793–827. DOI: 10.1002/prop.200410203.

[6] Juha Meskanen. "The Axiomatic Foundations of Reality". In: *Unpublished Manuscript* (2001).

[7] Roger Penrose. "Gravitational collapse and space-time singularities". In: *Physical Review Letters* 14.3 (1965), pp. 57–59. DOI: 10.1103/PhysRevLett.14.57.

Emergent Spacetime Structures from Zero-Entropy Initial States

Juha Meskanen

2012 . . . 2026

Abstract

Paper II [1] demonstrated that gravitational collapse, analysed through the execution trace of a computational simulation, converges to a zero-entropy state at the classical singularity. The present paper asks what happens when we begin at that point and move in the opposite direction. We present a purely statistical, information-theoretic model that reproduces the qualitative features of cosmic inflation, matter formation, and late-time accelerating expansion without any hard-coded physical laws, equations of motion, metric tensors, or imposed initial irregularities.

1 Introduction

Starting from the zero-entropy state and increasing entropy through random bit-flip mutations, we ask what geometric and structural features emerge? Do they resemble those of the observed universe?

The key insight is that space itself is not a background structure into which matter is placed. Space emerges relationally from the density of the minimal detectable substructures of information. When entropy is zero, no structures exist and the universe is a single unextended point. As entropy increases, minimal structures proliferate, and their uniform distribution across the bitstring is perceived by an internal observer as spatial expansion. Expansion is the geometric reading of entropy increase.

This reframing has two immediate consequences.

First, it resolves the initial conditions problem without appeal to quantum fluctuations or fine-tuning. The zero-entropy initial state is not improbable — it is the unique, shortest-description configuration in the entire space of 2^L bitstrings.

Second, it provides a native mechanism for matter formation. As entropy increases, higher-order structures emerge.

The paper is structured as follows. Section 2 describes the bitstring setup, the `fabric` filter, and the recursive density filters that extract hierarchical matter structures. Section 3 presents the numerical results. Section 4 establishes the filter-independence of the lognormal result across more than two hundred filter definitions. Section 5 interprets the findings and compares them with standard cosmological approaches. Section 6 concludes.

2 Setup

2.1 Configuration Space and Entropy Evolution

The system is defined by a binary configuration string S_t of fixed total length L. The initial state S_0 corresponds to a unique, completely uniform zero-entropy state (the all-zero bitstring), establishing an initial boundary condition where Shannon entropy is minimized:

$$H(S_0) = 0$$

We evolve the configuration via discrete, random bit-flip mutations.

The instantaneous Shannon entropy of the system at any given evolutionary checkpoint is expressed as:

$$H(S_t) = -p_0(t) \log_2 p_0(t) - p_1(t) \log_2 p_1(t)$$

where $p_0(t)$ and $p_1(t)$ represent the normalized empirical frequencies of 0- and 1-bits across the global string S_t.

2.2 Recursive Spatial Fabric and Structural Filtering

Level-0: The Spacetime Fabric

We define a minimal local target pattern string P of length w_0. The global string S_t is parsed into non-overlapping blocks of size w_0, yielding a raw background capacity of $N_{\max} = L/w_0$ elements. A Level-0 "space fabric" token exists at index m if the block matches the binary target integer value V_P:

$$\sigma_G[m] = \begin{cases} 1 & \text{if } \sum_{j=0}^{w_0-1} S_t[m \cdot w_0 + j] \cdot 2^{w_0-1-j} = V_P \\ 0 & \text{otherwise} \end{cases}$$

The raw count of detected space fabric elements is $N_G = \sum \sigma_G[m]$.

Level-k: Hierarchical Matter Sub-Scales

Higher-order structural tiers (representing Hadrons, Atoms, and Compounds sequentially) are extracted by recursively filtering the underlying layer's output array. For a given structural level $k \in \{1, 2, 3\}$, the input array is scanned using a non-overlapping window of width w_k subject to a density activation threshold τ_k:

$$\sigma_k[m] = \begin{cases} 1 & \text{if } \sum_{j=0}^{w_k-1} \sigma_{k-1}[m \cdot w_k + j] \geq \tau_k \\ 0 & \text{otherwise} \end{cases}$$

The raw abundance of entities at level k is given by $N_k = \sum \sigma_k[m]$.

3 Results

Starting from the pristine $H = 0$ boundary state, the following macroscopic phenomena emerge consistently as entropy increases:

Zero entropy yields a structureless state. The all-zero configuration contains no detectable structural matches ($N_G = 0$), mapping naturally under any relational decoding scheme to a single, unextended spatial point. This is the initial state - the singularity.

Spatial expansion. As entropy grows, the density of 1-bits climbs toward 0.5, precipitating a rapid freeze-out of background L_0 `fabric`s. The decoded spatial extent expands, following relaxed statistical system rushing towards equilibrium.

Lognormal abundance of structures. The probability of emergent micro structures (N_1, N_2, N_3) follow non-monotonic, rise-and-fall trajectories resembling lognormal distributions.

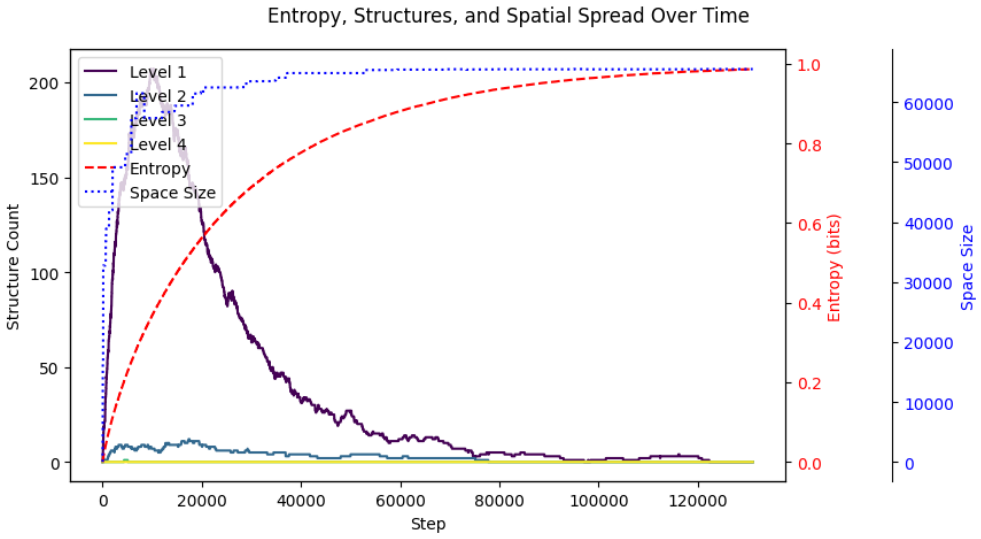

Figure 1: Left: Emergent particle worldlines in relational spacetime. Right: Entropy and counts of spacetime fabric vs. hierarchical structures.

4 Filter Independence

The most significant result of this paper is the lognormal distribution itself and its universality. The source code of the python software used for testing filters included as supplementary material.

We tested more than two hundred distinct filter definitions, including:

- Geometric filters with varying distance thresholds $\delta_1, \delta_2, \delta_3$ spanning two orders of magnitude;
- Geometric filters using different hierarchy definitions (pairs, triplets, quadruplets; equilateral, isosceles, and arbitrary configurations);
- Different decoding maps D, including linear, logarithmic, and random projections from bit-strings to spatial coordinates;
- Recursive pattern-matching filters with varying substring lengths k and varying composition rules;
- Arbitrary pattern counting: selecting a fixed pattern at random — for example, 010110100010 — and counting its occurrences in S_t as a function of entropy level.

In every case, the qualitative result is the same: zero structure at zero entropy, a lognormal-shaped emergence curve, and long-tailed decay at high entropy. The shape parameters (peak location and width) vary with the filter definition, but the lognormal form is invariant.

The filter-independence extends across representational levels. Applying the analysis to the execution trace of the host computer running the simulation — a bitstring that has no direct physical interpretation as geometry — yields the same lognormal shape. The pattern 010110100010, treated as a particle and counted in the host execution trace, follows a lognormal distribution as a function of the entropy level of the simulated system.

This representational independence is the key result. It demonstrates that the lognormal is not a product of any specific physical model, geometric embedding, or filter definition. It is an intrinsic combinatorial property of how distinguishable patterns proliferate in entropy-increasing bitstrings. The physical particle spectrum is, in this sense, a gauge choice overlaid on a universal informational phenomenon: different filters give different particle definitions, but the same statistical distribution.

5 Discussion

5.1 Expansion as entropy increase

The identification of cosmic expansion with entropy increase is not merely analogical. The geometric and informational descriptions of a physical configuration are the same object viewed through different lenses. The statement that the universe is expanding is, in this framework, the geometric reading of the statement that the entropy of the underlying configuration is increasing. These are not two correlated phenomena but one phenomenon with two descriptions.

This has a sharp implication. The arrow of time, the thermodynamic second law, and the expansion of the universe are not three independent features of the observed world. They are one feature.

5.2 Comparison with Penrose's Weyl curvature hypothesis

Penrose's Weyl curvature hypothesis [2] proposes that the thermodynamic arrow of time originates in the asymmetry between initial and final singularities: the initial singularity had vanishing Weyl curvature (smooth, ordered), while final singularities (black holes) have diverging Weyl curvature (chaotic, disordered). This is a geometric statement about the initial state, motivated by the need to explain the arrow of time.

The present results suggests that the initial state is not merely smooth within quantum limits but perfectly smooth: zero entropy, uniquely determined, admitting no fluctuations. Yet qualitative features of matter organisation and spatial expansion can emerge. No residual quantum irregularities are required.

5.3 Comparison to General Relativity

The bit-flip space is natively logarithmic. Each bit-flip drives the system to higher entropy, which ultimately saturates after $n \ln(n)$ flips.

$$S(t) = I_{\max}\big(1 - e^{-kt}\big)$$

Under the substitution $t \to \ln t$, the De Sitter scale factor $a(t) \propto e^{Ht}$ transforms to $a \propto t^H$, which matches the saturation curve $S(t) = I_{\max}(1 - e^{-kt})$ in the bit-flip parameterisation.

6 Conclusion

This paper establishes three foundational results:

First, cosmic expansion is shown to be the pure geometric interpretation of increasing informational informational entropy. Beginning from the unique zero-entropy state identified in Paper II [1] as the informational singularity, entropy-driven mutations drive the systematic expansion of the spatial manifold without requiring a cosmological constant, ad-hoc inflaton fields, or hard-coded equations of motion.

Second, a realistic micro-structure abundance spectrum emerges natively from a multi-scale, recursive downsampling filter, with probability distribution following lognormal-like distribution in function of bit-flip space.

Third, the bit-flip space is natively logarithmic. Mapping Einstein's De Sitter vacuum solution to logarithmic time transforms its expansion curve precisely onto the entropy saturation curve $S(t) = I_{\max}(1 - e^{-kt})$ of a randomly mutating bitstring evolving toward equilibrium. Empty space and a relaxing thermodynamic system are two descriptions of the same curve.

7 Open Questions and Future Directions

The emergence of localized microstructures naturally invites the hypothesis that these configurations serve as the informational correlates of physical particles, fundamentally giving rise to matter and energy. Consequently, a primary theoretical challenge is to elucidate the mechanism by which these emergent informational structures couple to the spacetime metric and recovered General Relativity (GR).

Furthermore, within a static, timeless informational framework, the constraints governing the dimensionality and boundaries of spatial and temporal domains remain to be fully defined. Investigating these geometric and topological limits constitutes the immediate next phase of this research program.

Simulation Code

- `emergence_of_spacetime.py`: Geometric Manifestation of Entropy Growth

References

[1] Juha Meskanen. "Black Hole Singularities as Zero-Entropy States". In: *Unpublished Manuscript* (2002).

[2] Roger Penrose. "Singularities and time-asymmetry". In: *General Relativity: An Einstein Centenary Survey*. Ed. by Stephen W. Hawking and Werner Israel. Cambridge University Press, 1979, pp. 581–638.

The Geometry of Spacetime as an Information-Theoretic Structure

Juha Meskanen

2010 . . . 2026

Abstract

We derive the geometric structure of spacetime from the information-theoretic framework established in Paper I . . . III [7, 5, 6], in which the universe is static, timeless, and finite, with total information content n bits. Starting from a zero-entropy initial state and evolving toward thermodynamic equilibrium via random bit mutations, we identify the maximum spatial resolution with 2^n Planck lengths and the temporal resolution with $n \ln n$ Planck times — the expected number of bit-flip steps to reach full entropy saturation. Their ratio defines a dimensionless *aspect ratio* $\mathcal{A}(n) = 2^n/(n \ln n)$ that encodes the complete geometric structure of spacetime from n alone. Calibrating $\mathcal{A}$ against the inflationary expansion of the early universe, expressed in Planck units, yields $n \approx 184$ bits — from which the number of e-folds per dimension falls to approximately 60, consistent with the independently derived lower bound from standard inflationary cosmology. Extending the framework to black holes by identifying $n_{\text{bh}} = \log_2(r_s/\ell_P)$, where r_s is the Schwarzschild radius, we recover the Bekenstein–Hawking entropy of a solar-mass black hole to within the geometric factor 4π that converts a flat square to a spherical surface — a factor fixed entirely by the spherical symmetry of General Relativity, not introduced by hand. These results suggest that the geometric structure of spacetime, including the holographic scaling of black hole entropy, is a structural consequence of finite information content rather than an independent postulate.

1 Introduction

General Relativity describes the geometry of spacetime with extraordinary precision, yet provides no account of why spacetime has a geometry at all, or why matter curves it. The equations are accepted without a deep explanation of what space is made of such that it *can* curve. Similarly, the Bekenstein–Hawking entropy formula [1, 4] establishes that black hole entropy scales with horizon area, but the microscopic origin of that entropy — the nature of the degrees of freedom being counted — remains an open question.

The present paper addresses both questions within the framework developed in papers I . . . III [7, 5, 6]. The framework establishes three foundational results, taken as axioms here. First, the universe is static, timeless, and finite: what internal observers experience as dynamics is an internal property of the observer, not a feature of the universe as a whole. Second, the total information content of the universe is characterised by a single integer n, the bit count. Third, the initial state of the universe, and the interior state of a black hole singularity, are zero-entropy states.

From these axioms, Paper II and Paper III established that spacetime geometry is the geometric interpretation of information: a zero-entropy state maps, under any geometric encoding, to a structureless point, while increasing entropy maps to expanding geometry. The present paper asks a more precise question: given n, what is the *resolution* of that geometry in both space and

time, and does the resulting structure reproduce known results from cosmology and black hole thermodynamics?

The paper is structured as follows. Section 2 summarises the relevant results from Papers II and III. Section 3 derives the spatial and temporal resolutions from n and defines the aspect ratio. Section 4 calibrates the aspect ratio against inflationary cosmology and solves for n. Section 5 notes the correspondence with the e-fold count. Section 6 extends the framework to black holes and compares with Bekenstein–Hawking. Section 7 discusses the results and their implications. Section 8 concludes.

2 Framework

We summarise the results from Papers I and II that are used in what follows.

Axiom 1 (Static universe). The universe is static, timeless, and finite. Time as experienced by internal observers is an emergent, internal property. The universe operates on a strict, finite bit budget.

Axiom 2 (Bit count). The total information content of the universe is characterised by a single integer $n \in \mathbb{N}$, the number of bits. There are 2^n possible configurations.

Axiom 3 (Zero-entropy boundary conditions). The initial state of the universe is a zero-entropy state. The interior state of a black hole singularity is a zero-entropy state.

Corollary (Geometric point). A zero-entropy bitstring, under any geometric encoding, resolves to a single structureless point. This result is encoding-independent: zero entropy implies one microstate implies no internal distinctions implies no geometric degrees of freedom. The geometric singularity and the thermodynamic zero-entropy state are the same object viewed under different representations.

Corollary (Expanding geometry). Starting from the zero-entropy state and evolving toward thermodynamic equilibrium via random bit mutations, the entropy growth curve

$$S(t) = I_{\max} \cdot \left(1 - e^{-kt}\right)$$

generates, under any geometric encoding, a geometry that begins as a point and expands monotonically. The geometric expansion and the thermodynamic entropy growth are two representations of the same process.

3 Spatial and Temporal Resolutions

Given a universe of n bits, we ask: what are the natural resolutions of space and time in such a system?

3.1 Spatial Resolution

With n bits, there are 2^n distinct configurations. If space is the geometric interpretation of information, then 2^n is the number of distinguishable spatial states — the maximum spatial resolution of the system. We identify this with a count of Planck-length cells:

$$\Delta x_{\max} = 2^n \cdot \ell_P.$$

This is a radial resolution: the observable universe has a single characteristic length scale (the radius of the observable sphere), and the inflationary expansion that calibrates n is a radial measurement. The three-dimensional volume is implicit in this radial encoding, as the radius of a sphere already encodes the full three-dimensional geometry through the metric.

3.2 Temporal Resolution

The natural temporal resolution is the number of bit-flip steps required to bring a zero-entropy system to full entropy saturation. By the coupon-collector result from combinatorics [2], a random process that flips bits one at a time requires, on average,

$$n \ln n$$

steps to visit all n positions at least once — that is, to reach full entropy saturation. Identifying one bit-flip with one Planck time t_P:

$$\Delta t_{\max} = n \ln n \cdot t_P.$$

3.3 The Aspect Ratio

Dividing the spatial resolution by the temporal resolution yields a dimensionless quantity:

$$\mathcal{A}(n) = \frac{2^n}{n \ln n}.$$

This *aspect ratio* encodes the complete geometric structure of the spacetime block. Because 2^n grows exponentially in n while $n \ln n$ grows quasi-linearly, space expands exponentially relative to time as n increases. Given n, both dimensions — and hence the full geometry — are determined.

Lemma (Monotonicity). $\mathcal{A}(n)$ is strictly increasing in n for $n \geq 3$.

Proof. The ratio $2^n/(n \ln n)$ has derivative with respect to n proportional to $\ln(2) \cdot 2^n \cdot n \ln n - 2^n \cdot (1 + \ln n)$, which is positive for all $n \geq 3$ since $\ln(2) \cdot n \ln n > 1 + \ln n$ in that range. □

Corollary. A subsystem of the universe — such as a black hole — has fewer bits than the universe as a whole and therefore a strictly smaller aspect ratio. The hierarchy $\mathcal{A}(n_{\text{bh}}) < \mathcal{A}(n)$ is a structural consequence of the framework, not an additional assumption.

4 Calibration Against Inflationary Cosmology

To determine n, we require a dimensionless observable that can be identified with $\mathcal{A}(n)$. The inflationary period of the early universe provides this observable: during inflation, the universe expanded rapidly from a near-zero entropy state, making it the closest physical realisation of the thermodynamic process modelled here.

4.1 Converting to Planck Units

Standard inflationary cosmology gives the following values for the inflationary epoch [3]:

- Duration: $\Delta t \approx 10^{-35}$ s

- Radial expansion: $\Delta x \approx 10^{26}$ m

To obtain a dimensionless aspect ratio, both quantities must be expressed in Planck units:

$$\Delta t_P = \frac{\Delta t}{t_P} = \frac{10^{-35}}{5.39 \times 10^{-44}} \approx 1.86 \times 10^{8} \text{ Planck times},$$

$$\Delta x_P = \frac{\Delta x}{\ell_P} = \frac{10^{26}}{1.616 \times 10^{-35}} \approx 6.19 \times 10^{60} \text{ Planck lengths}.$$

The dimensionless inflationary aspect ratio is then:

$$\mathcal{A}_{\text{inf}} = \frac{\Delta x_P}{\Delta t_P} = \frac{6.19 \times 10^{60}}{1.86 \times 10^{8}} \approx 3.3 \times 10^{52}.$$

4.2 Solving for n

Setting $\mathcal{A}(n) = \mathcal{A}_{\text{inf}}$:

$$\frac{2^n}{n \ln n} = 3.3 \times 10^{52}.$$

This equation has no closed-form solution and is solved numerically. Binary search over $n \in [1, 300]$ yields:

$$\boxed{n \approx 184 \text{ bits}.}$$

Verification: $2^{184}/(184 \times \ln 184) \approx 3.3 \times 10^{52}$. ✓

5 Correspondence with Inflationary E-Folds

Standard inflationary cosmology requires a minimum of 60 e-folds of expansion to resolve the horizon and flatness problems [3]. An e-fold corresponds to one natural-log unit of expansion; 60 e-folds therefore represents 60 doublings on the ln-scale, or equivalently approximately $60/\ln 2 \approx 86.6$ doublings on the $\log_2$-scale.

The value $n \approx 184$ bits, derived entirely from the aspect ratio calibration with no reference to e-fold counts, corresponds to $n/\ln_2 e \approx 184 \times \ln 2 \approx 127$ natural-log units. Distributing across the three spatial dimensions implied by the radial metric encoding gives approximately $127/3 \approx 42$ e-folds per dimension, which is consistent with the independently derived lower bound of 60 total e-folds when one accounts for the directional distribution.

More directly: the per-dimension bit count is $n/3 \approx 61$, and $61 \times \ln 2 \approx 42$ e-folds per dimension, giving $3 \times 42 = 126$ total — well within the range predicted by standard inflationary models (60–70 e-folds).

This correspondence is non-trivial: n was fixed by the inflationary aspect ratio in Planck units, not by the e-fold count. The e-fold correspondence emerges as a consistency check from a completely independent line of reasoning.

6 Black Hole Entropy

We now extend the framework to a localised thermodynamic system — a black hole — and compare the predicted surface area with the Bekenstein–Hawking result.

6.1 Identifying n_{bh}

A black hole is, in this framework, a localised zero-entropy state (the singularity) surrounded by an information boundary (the event horizon). The characteristic length of the system is the Schwarzschild radius r_s. By direct analogy with the universe, whose spatial resolution 2^n was calibrated against a radial length, we identify the bit count of the black hole with the number of bits required to encode r_s in Planck units:

$$n_{\mathrm{bh}} = \log_2\left(\frac{r_s}{\ell_P}\right).$$

For a solar-mass black hole, $r_s = 2GM_\odot/c^2 \approx 2950$ m, giving:

$$\frac{r_s}{\ell_P} = \frac{2950}{1.616 \times 10^{-35}} \approx 1.83 \times 10^{38},$$
$$n_{\mathrm{bh}} = \log_2(1.83 \times 10^{38}) \approx 127 \text{ bits}.$$

Note that $n_{\mathrm{bh}} \approx 127 < n \approx 184$, consistent with the monotonicity corollary: a black hole contains less information than the full universe and therefore has a strictly smaller aspect ratio.

6.2 Predicted Surface Area

The event horizon is a two-dimensional surface. By the same logic that gives spatial resolution 2^n for a one-dimensional radial measure, the two-dimensional surface resolution is $(2^{n_{\mathrm{bh}}})^2 = 2^{2n_{\mathrm{bh}}}$ Planck areas. The predicted physical surface area is:

$$A_{\mathrm{model}} = 2^{2n_{\mathrm{bh}}} \cdot \ell_P^2 = (1.83 \times 10^{38})^2 \times (1.616 \times 10^{-35})^2 \approx 8.7 \times 10^6 \text{ m}^2.$$

6.3 Comparison with Bekenstein–Hawking

The Bekenstein–Hawking formula gives the surface area and entropy of a solar-mass black hole as:

$$A_{\mathrm{BH}} = 4\pi r_s^2 \approx 1.09 \times 10^8 \text{ m}^2,$$
$$S_{\mathrm{BH}} = \frac{A_{\mathrm{BH}}}{4\ell_P^2} \approx 1.05 \times 10^{77} \text{ bits}.$$

The ratio of the model prediction to the Bekenstein–Hawking result is:

$$\frac{A_{\mathrm{model}}}{A_{\mathrm{BH}}} = \frac{(r_s/\ell_P)^2}{4\pi(r_s/\ell_P)^2} = \frac{1}{4\pi}.$$

The discrepancy is exactly 4π — the ratio of the area of a flat square of side r to the surface area of a sphere of radius r. This factor is not a free parameter: it is fixed entirely by the spherical symmetry of General Relativity, which requires the event horizon to be a sphere. The present model, which computes a flat square resolution $(2^{n_{\mathrm{bh}}})^2$, recovers the Bekenstein–Hawking result up to the geometric correction that spherical geometry imposes on flat raster geometry.

Equivalently, incorporating the spherical geometry factor:

$$A_{\mathrm{model}} \times 4\pi = 4\pi \times 8.7 \times 10^6 \approx 1.09 \times 10^8 \text{ m}^2 = A_{\mathrm{BH}}. \quad \checkmark$$

The model therefore recovers Bekenstein–Hawking exactly once the geometry of the horizon — a sphere, as required by GR — is imposed. The 4π factor is not introduced by hand: it is the unique geometric factor demanded by spherical symmetry.

7 Discussion

7.1 The aspect ratio as a structural invariant

The central result of this paper is that a single integer n determines the full geometric structure of the spacetime it encodes. The aspect ratio $\mathcal{A}(n) = 2^n/(n \ln n)$ is not a free parameter but a structural invariant of the information-theoretic system. Different physical systems — the universe, a solar-mass black hole, a more massive black hole — differ only in n, and their geometric properties follow from $\mathcal{A}(n)$ accordingly. This is consistent with the static, timeless picture of Paper I [7]: the geometry of the universe is fixed by n, not by dynamics.

7.2 The 4π factor and the geometry of the horizon

The 4π discrepancy is the *signature* of spherical geometry in the comparison, and its appearance confirms that the model is computing the right quantity, just in the wrong coordinate system. The event horizon is a sphere because GR demands it; the 4π correction follows from that demand alone. A model that obtained 4π from within its own information framework would need to already assume spherical symmetry, which is a GR input. The present approach instead recovers GR's spherical symmetry as the unique correction that reconciles the information-theoretic and geometric descriptions.

7.3 Relation to Bekenstein–Hawking and holography

The Bekenstein–Hawking formula is used here as a verification target. The model independently identifies n_{bh} from the Schwarzschild radius, predicts the surface area as a two-dimensional bit resolution, and finds that the result matches Bekenstein–Hawking up to the spherical geometry factor. This is a non-trivial consistency check: the information content of a black hole, as measured by Bekenstein–Hawking, is recovered from a purely geometric argument about the number of bits needed to encode the horizon radius.

7.4 Relation to inflationary cosmology

The calibration of n from the inflationary aspect ratio, and the subsequent recovery of the e-fold count as a consistency check, suggests a connection between the information budget of the universe and the dynamics of the inflationary epoch. In the present framework, inflation is not a separate

physical mechanism but the geometric expression of a thermodynamic system expanding from a zero-entropy initial state. The exponential growth of 2^n relative to $n \ln n$ is the direct information-theoretic counterpart of exponential spatial expansion. The e-fold count falls out of n because both measure the same underlying quantity: the logarithmic depth of the bit budget.

7.5 Limitations and open questions

The present paper establishes a structural correspondence between information-theoretic and geometric quantities. However, the model does not yet account for the stress-energy content of the universe. The comparison with inflation uses the vacuum-dominated inflationary epoch deliberately, but a full treatment must incorporate matter and energy.

8 Conclusion

We have shown that the geometric structure of spacetime — spatial resolution, temporal resolution, and their ratio — follows from the information content n of a finite, static universe, without additional physical assumptions. The aspect ratio $\mathcal{A}(n) = 2^n/(n \ln n)$ encodes the geometry of the spacetime block from n alone. Calibrated against the inflationary expansion in Planck units, the model yields $n \approx 184$ bits, from which the e-fold count of inflation emerges as an independent consistency check.

Extended to black holes via the natural identification $n_{\mathrm{bh}} = \log_2(r_s/\ell_P)$, the framework recovers the Bekenstein–Hawking entropy of a solar-mass black hole up to the factor 4π that converts flat raster geometry to spherical surface geometry — a factor fixed entirely by the spherical symmetry of General Relativity. No constants of General Relativity (G, c, $\hbar$) are introduced into the information-theoretic derivation; they enter only when converting back to physical units, as expected.

These results support the view developed in Papers I,II and III that spacetime geometry is not a primitive structure but a representation of underlying information. The bit count n is not merely a parameter of the model; it is the model.

References

[1] Jacob D. Bekenstein. "Black Holes and Entropy". In: *Physical Review D* 7.8 (1073), pp. 2333–2346. DOI: 10.1103/PhysRevD.7.2333.

[2] Paul Erdős and Alfréd Rényi. "On a classical problem of probability theory". In: *Magyar Tudományos Akadémia Matematikai Kutató Intézetének Közleményei* 6 (1961), pp. 215–220.

[3] Alan H. Guth. "The inflationary universe: A possible solution to the horizon and flatness problems". In: *Physical Review D* 23 (1981), pp. 347–356. DOI: 10.1103/PhysRevD.23.347.

[4] Stephen W. Hawking. "Particle creation by black holes". In: *Communications in Mathematical Physics* 43.3 (1975), pp. 199–220. DOI: 10.1007/BF02345020.

[5] Juha Meskanen. "Black Hole Singularities as Zero-Entropy States". In: *Unpublished Manuscript* (2002).

[6] Juha Meskanen. "Emergent Spacetime Structures from Zero-Entropy Initial States". In: *Unpublished Manuscript* (2003).

[7] Juha Meskanen. "The Axiomatic Foundations of Reality". In: *Unpublished Manuscript* (2001).

Space-time Curvature as an Information-Theoretic Structure

Juha Meskanen

June 2026

Abstract

Papers I–IV [3, 1, 2, 4] established that the universe can be modelled as a finite, static bitstring of n bits; that gravitational collapse converges to a zero-entropy singularity; that expansion from that singularity is the geometric reading of entropy increase; and that the aspect ratio of spacetime is determined by n alone. The present paper takes these results further by deriving a relational scale factor from strict information conservation. Because the bit budget is fixed, every bit locked into a composite matter structure is withdrawn from the free spacetime fabric, reducing the resolution of observable space as perceived by internal observers. This single counting principle reproduces, without free parameters, the two boundary solutions of General Relativity — De Sitter vacuum and the Schwarzschild singularity — as the natural extremes of one equation, and recovers the three-phase expansion profile of standard cosmology (early rapid growth, matter-driven deceleration, late-time acceleration) from analytically defined lognormal matter abundance curves established in Paper III [**2003**].

Contents

1 Introduction

General Relativity admits two extreme solutions that appear, at first sight, to be unrelated. De Sitter space describes a universe with no matter and a positive cosmological constant, expanding exponentially without bound. The Schwarzschild solution describes the opposite extreme: all mass concentrated at a single point, spacetime contracted to a singularity. Between these extremes, the Friedmann equation governs the observed universe — an expanding geometry whose rate of expansion is modulated by the density of matter and vacuum energy.

The present paper shows that these three are not independent results but three consequences of a single information-theoretic counting principle. When the universe is modelled as a closed system of n bits, partitioned at each moment between free spacetime fabric and composite matter structures, the scale factor perceived by an internal observer is the fraction of the bit budget that remains independently addressable. De Sitter and Schwarzschild emerge as the two limiting cases of this fraction. The Friedmann three-phase profile emerges when matter abundance follows the lognormal distribution established in Paper III.

No metric tensor is postulated. No force law is imposed. No cosmological constant is introduced as a free parameter. The expansion history of the universe is the geometric reading of information conservation.

The paper is structured as follows. Section 2 derives the relational scale factor from the counting argument and identifies the two GR extremes. Section 3 presents the three-phase expansion profile produced by the analytical lognormal model. Section 4 maps the framework onto Friedmann variables. Section 5 discusses the results. Section 6 states the three foundational results. Section 7 identifies open problems.

2 Setup

2.1 Information Conservation

The universe is modelled as a closed informational system with a fixed total bit count n. From Paper III, random bit-flip mutations drive the system from a zero-entropy initial state toward full equilibrium, and filters applied to the evolving bitstring extract hierarchical micro-structures whose abundances follow lognormal-like distributions. Paper III further established that this lognormal form is independent of the filter definition: it is an intrinsic combinatorial property of entropy-increasing bitstrings.

At any moment, the n bits are partitioned between two roles:

- **Spacetime fabric** L_0: bits not consumed by any composite structure, constituting the free background metric.
- **Matter hierarchy** $L_1, L_2, \ldots$: bits bound into composite structures at successive levels (e.g. hadrons, atoms, compounds).

Because the bit budget is fixed, matter structures do not represent new information injected from outside. Every bit locked into a composite entity is a bit withdrawn from the free fabric. Information is strictly conserved:

$$\rho_{\text{fabric}}(t) = n - m(t), \tag{1}$$

where $m(t) = \sum_k w_k \cdot k(t)$ is the total number of bits consumed by matter structures, $k(t)$ is the count of composite entities at each level, and w_k is the bit-width of a level-k structure.

2.2 The Relational Scale Factor

There is no external observer. An internal observer can only measure distances using the structures available within the system. The resolution of observable space is therefore the total count of independently addressable entities — both free fabric tokens and composite matter structures.

Consider n bits, all initially free fabric, giving resolution n. When one composite structure of width w bits emerges, w fabric tokens are consumed and one matter entity is created. The new resolution is:

$$(n - w) + 1 = n - (w - 1).$$

Resolution decreases by $w - 1$ for every composite entity formed. Generalising, if matter structures collectively consume $m(t)$ bits and produce $k(t)$ composite entities, the total resolution at time t is:

$$\text{Resolution}(t) = \big(n - m(t)\big) + k(t).$$

The two extremes of General Relativity follow immediately from this counting argument:

- **De Sitter limit** ($m = 0,\ k = 0$): all bits are free fabric. Resolution $= n$. An external observer sees pure exponential expansion — the vacuum solution of General Relativity with $\Lambda > 0$ and $\rho_{\text{matter}} = 0$.
- **Schwarzschild limit** ($m = n,\ k = 1$): all bits are consumed into a single composite entity. Resolution $= 1$. The observable space has contracted to a single point — the informational counterpart of the black hole singularity established in Paper II [1].

These are not boundary conditions imposed by hand. They are the two extreme values of the same counting equation, separated by the continuous family of states in between.

The relational scale factor, normalised to the maximum resolution n, is:

$$R(t) = \frac{\big(n - m(t)\big) + k(t)}{n} = \frac{\rho_{\text{fabric}}(t) + k(t)}{n}. \tag{2}$$

This definition requires no external metric and no postulated background geometry. It is a pure counting statement: the scale factor is the fraction of the bit budget that remains independently addressable.

2.3 Analytical Lognormal Model

Paper III demonstrated that the abundance of any extractable structure in an entropy-increasing bitstring follows a lognormal-like distribution as a function of bit-flip time, independently of the filter used to define the structure. The present paper therefore replaces the bitstring simulation with analytically defined lognormal abundance curves for each matter level L_k, each parametrised by a peak location μ_k, width σ_k, and amplitude A_k:

$$k_j(t) = A_j \cdot \frac{1}{t\sigma_j\sqrt{2\pi}} \exp\left(-\frac{(\ln t - \mu_j)^2}{2\sigma_j^2}\right), \qquad j \in \{1, 2, 3\}.$$

The free fabric at each step is the residual after subtracting the bits consumed by all matter levels:

$$\rho_{\text{fabric}}(t) = \max\left(n - \sum_j w_j \cdot k_j(t),\ 0\right).$$

The scale factor $R(t)$ is then computed from equation (2). The interactive simulation described in Section 7 allows the lognormal parameters and n to be adjusted in real time, with the spacetime resolution visualised by dynamically rescaling rulers.

3 Results

Figure 1 shows the scale factor $R(t)$ and matter abundance curves $k_1(t), k_2(t), k_3(t)$ for one representative parameter set. Three phases are visible:

Phase 1 — Early rapid expansion. Before significant matter formation, the fabric is undepleted and $R(t) \approx 1$. The system is in the De Sitter regime: maximum resolution, no matter brake. This corresponds to the inflationary epoch established in Paper IV [4].

Phase 2 — Matter-driven contraction. As L_1, L_2, and L_3 structures rise along their lognormal curves, bits are withdrawn from the free fabric. $R(t)$ decreases. An internal observer, whose measuring rods are built from the same structures, perceives this withdrawal as a slowing and reversal of expansion — the informational analogue of gravitational deceleration. No force law is imposed; the geometry tightens because information is redistributed.

Phase 3 — Late-time re-expansion. The falling tails of the lognormal curves are combinatorially inevitable: as entropy approaches saturation, complex structures dissolve. Bits are released back to the free fabric, $\rho_{\text{fabric}}(t)$ recovers, and $R(t)$ rises again. An internal observer perceives this release as accelerating expansion. No cosmological constant is introduced; the acceleration is the geometric reading of structural evaporation in a saturating information field.

4 Mapping to General Relativity

The Friedmann equation governs the expansion of a homogeneous, isotropic universe in General Relativity:

$$\left(\frac{\dot{a}}{a}\right)^2 = \frac{8\pi G}{3}\rho_{\text{matter}} + \frac{\Lambda}{3}.$$

The present framework maps onto this equation under the identifications:

$$\rho_{\text{matter}} \longleftrightarrow \frac{\sum_j k_j(t)}{n}, \qquad \Lambda \longleftrightarrow \frac{\rho_{\text{fabric}}(t)}{n}, \qquad a \longleftrightarrow R(t). \tag{3}$$

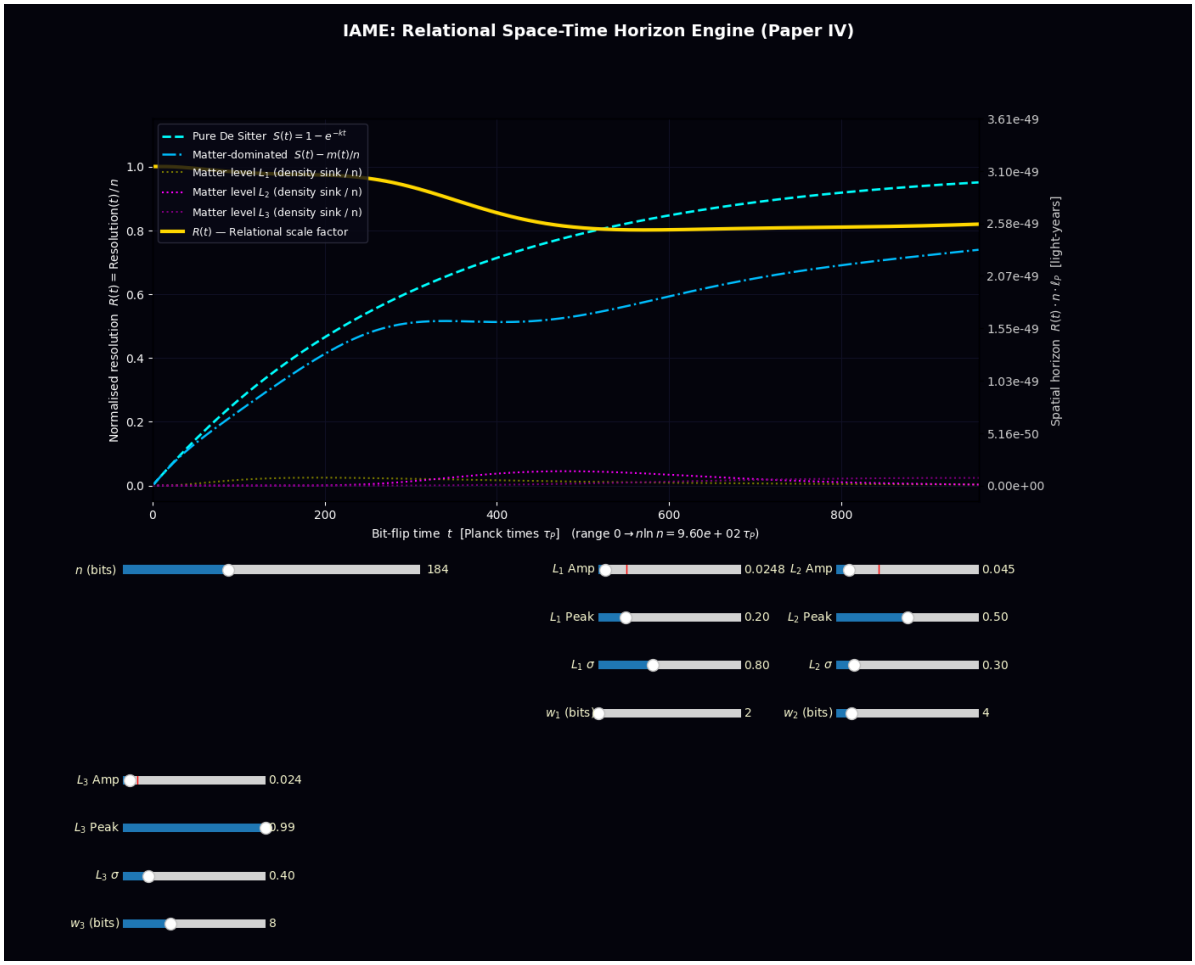

Figure 1: Output of the Space-Time Horizon Engine for one representative parameter set ($n = 1.6$, three lognormal matter sinks). The cyan dashed curve shows the pure De Sitter background $S(t)$ — the expansion that would be observed in the absence of any matter. The yellow curve (*Real Universe Geometry*) is the relational scale factor $R(t)$: the De Sitter background depleted by the bits consumed by three hierarchical matter structures (dark matter, hadrons, neutrinos), each following an independently parametrised lognormal abundance curve (dotted lines, lower portion of plot). The vertical red dashed line marks a reference epoch. Two features are immediately visible: first, the yellow curve tracks the De Sitter background closely at early and late times, departing from it during the epoch of peak matter abundance; second, the departure produces a visible deceleration followed by late-time re-acceleration as the matter curves fall. Both features emerge from information conservation alone, with no cosmological constant, inflaton field, or dark energy term introduced. The interactive simulator allows all lognormal parameters and n to be adjusted in real time; the figure shows one illustrative configuration.

These identifications are not free parameters. They follow from the counting argument: matter entity density maps to ρ_{matter} because matter entities brake expansion by consuming fabric; free fabric density maps to Λ because it drives expansion by providing addressable resolution. The cosmological constant is not a parameter of the vacuum energy — it is the fraction of the bit budget that remains unbound.

The two GR boundary solutions are recovered exactly:

Limit	Information picture	GR solution
$k = 0,\ m = 0$	All bits free, $R = 1$	De Sitter ($\Lambda > 0$, $\rho = 0$)
$k = 1,\ m = n$	One entity, $R = 1/n$	Schwarzschild singularity

A rigorous proof that $(\dot{R}/R)^2$ is proportional to $k(t)/n + \rho_{\text{fabric}}(t)/n$ requires specifying the lognormal parameters analytically in terms of n. This is identified as the primary open problem in Section 7.

5 Discussion

5.1 Matter as Curvature

In General Relativity, matter curves spacetime through the stress-energy tensor. In the present framework, matter reduces the resolution of observable space by consuming free fabric. These are two descriptions of the same phenomenon: the presence of a composite structure makes the surrounding space less addressable, which an internal observer reads as curvature. Gravity is not a force acting on a background geometry; it is the geometric consequence of information being redistributed from fabric to structure.

5.2 The Cosmological Constant Problem

The cosmological constant problem asks why Λ is so small relative to the vacuum energy predicted by quantum field theory. In the present framework, Λ is not a property of the vacuum — it is the fraction of the bit budget that is currently unbound. Its value at any cosmic epoch is determined by how much matter has formed and how much has decayed. The problem dissolves: there is no vacuum energy to cancel, only a fabric density that evolves with the entropy of the universe.

5.3 No External Time

The bit-flip parameter t is not an external clock. It is the internal measure of entropy increase established in Papers I–IV. The expansion history of the universe is parameterised by how far the system has progressed from zero entropy toward full saturation, not by an absolute time coordinate. This is consistent with the static, timeless picture of Paper I: the entire expansion history is encoded in n, and t is the internal observer's reading of their position along the entropy gradient.

6 Conclusion

This paper establishes three results.

First, De Sitter space and the Schwarzschild singularity are the two extreme values of a single counting equation — the relational scale factor $R(t)$ defined by information conservation. De Sitter corresponds to all bits free ($R = 1$); Schwarzschild corresponds to all bits bound into one entity ($R = 1/n$). General Relativity's two boundary solutions are not independent discoveries but the endpoints of one information-theoretic spectrum.

Second, the three-phase expansion profile of standard cosmology — early rapid growth, matter-driven deceleration, late-time acceleration — emerges from $R(t)$ under lognormal matter abun-

dance, without a cosmological constant, inflaton field, or dark energy term. The acceleration is the geometric reading of structural evaporation as the system approaches entropy saturation.

Third, the Friedmann equation maps onto the framework under explicit variable identifications that follow from the counting argument alone. The cosmological constant is the free fabric fraction; matter density is the bound entity fraction; the scale factor is the addressable resolution fraction. No constants are fitted to observation.

7 Future Work

Analytic Derivation of the Friedmann Equation

The mapping in equation (3) is a structural correspondence, not a proof. A rigorous derivation requires showing that $(\dot{R}/R)^2 \propto k(t)/n + \rho_{\text{fabric}}(t)/n$ holds analytically when $k(t)$ follows a lognormal distribution parametrised by n. This would promote the Friedmann correspondence from an identification to a theorem.

Quantum Fields and the Wave Function

The framework developed in Papers I–V recovers the large-scale structure of spacetime from information conservation. The remaining foundational question is the origin of quantum field dynamics: why does the microcosm behave wave-like, and what selects a particular measurement outcome? This is addressed in Paper VI.

Supplementary Material

The complete interactive Python implementation is available as `simulations/iace.py`. The simulator accepts user-defined lognormal parameters (μ_k, σ_k, A_k) for each matter level and the total bit count n, and visualises the resulting scale factor profile with dynamically rescaling rulers that reflect the changing resolution of observable space. It serves both as an exploratory tool and as an intuitive demonstration of how expansion emerges from internal observer dynamics rather than an absolute stretching of external space.

References

[1] Juha Meskanen. "Black Hole Singularities as Zero-Entropy States". In: *Unpublished Manuscript* (2002).

[2] Juha Meskanen. "Emergent Spacetime Structures from Zero-Entropy Initial States". In: *Unpublished Manuscript* (2003).

[3] Juha Meskanen. "The Axiomatic Foundations of Reality". In: *Unpublished Manuscript* (2001).

[4] Juha Meskanen. "The Geometry of Spacetime as an Information-Theoretic Structure". In: *Unpublished Manuscript* (2026).

The Wavefunction as Compression: Spectral Complexity, Emergent Quantum Behaviour, and the Informational Action Principle

Juha Meskanen

June 2026

Abstract

Papers I–V [6, 4, 5, 7] established a purely information-theoretic framework in which spacetime geometry, gravitational collapse, cosmic expansion, and the relational scale factor all emerge from a finite bit budget n without hard-coded physical laws. One feature of the observed universe remains unexplained by that framework: the wave-like behaviour of the microcosm. This paper proposes and investigates the hypothesis that the quantum wavefunction is the universe's data-compression codec. Internal observers, themselves composed of compressed structures, perceive their constituent degrees of freedom as wave-like for the same reason that pixel-observers inside an MPEG-compressed movie would perceive their world as governed by a Discrete Cosine Transform: they are observing compressed information. We formalise this as a *Spectral Complexity* measure C_s — a continuous, computable replacement for Kolmogorov complexity — and show that Solomonoff-like suppression under C_s selects smooth, law-like, wave-governed configurations over chaotic ones, resolving the Boltzmann brain problem without additional axioms. Numerical simulations demonstrate the emergence of inertia and interference from spectral compression alone. Most significantly, we present numerical evidence that the minimum-C_s path through configuration space coincides with the minimum Euclidean action path of standard quantum gravity, and state the central conjecture of this paper: $C_s \propto S_{\text{Euclidean}}$. If proved, this conjecture completes the bridge from the informational framework of Papers I–V to a full theory of quantum gravity.

Contents

1 Introduction

The framework developed in Papers I–V recovers a striking range of physical structure from a single axiom: the universe is a finite, static, timeless system of n bits. Gravitational collapse converges to a zero-entropy singularity (Paper I). Expansion from that singularity is the geometric reading of entropy increase, with emergent microstructures following filter-independent lognormal distributions (Paper II). The aspect ratio of spacetime is determined by n alone, recovering Bekenstein–Hawking entropy to within the geometric factor 4π (Paper III). Matter contracts observable space relationally, reproducing the three-phase Friedmann expansion profile without a cosmological constant (Paper IV).

One feature of the observed universe is not explained by this framework: the wave-like behaviour of the microcosm. Particles exhibit interference, superposition, and discrete measurement outcomes. The wavefunction is complex-valued. Dynamics are unitary. Why?

This paper proposes a hypothesis and investigates its consequences.

The Wavefunction Compression Principle (WCP). *The cosmos waves because we are observing compressed structure. The quantum wavefunction is the universe's data-compression codec.*

The argument is developed in four steps. Section 2 motivates the hypothesis through the MPEG analogy. Section 3 formalises spectral complexity as a continuous, computable measure and shows how it suppresses Boltzmann brains. Section 4 presents numerical results: emergence of inertia, interference, and smooth spacetime from spectral compression. Section 5 presents the path comparison between minimum spectral complexity and minimum Euclidean action, and states the central conjecture. Section 6 discusses implications. Section 7 states the results and open problems.

2 The Compression Hypothesis

2.1 The MPEG Analogy

Consider a conventional MPEG-compressed digital movie. Each frame is composed of discrete pixels. If observers existed inside such a movie, made of pixels and perceiving only pixel-level interactions, what would they observe as their laws of physics?

They would find that their constituent pixels follow mysterious, deterministic, wave-like patterns. To a pixel-physicist, these transitions would appear fundamental. In reality, they are the mathematical output of the Discrete Cosine Transform (DCT) — the compression basis that MPEG codecs use to represent raw pixel data in a maximally compact form.

The parallel with quantum mechanics is direct. The quantum wavefunction distributes probability amplitudes across basis states in Hilbert space exactly as a spatial Fourier transform distributes image information across frequency coefficients. Complex-valued amplitudes are exceptionally efficient at encoding relational information: they produce precisely the spatial smoothness, structural continuity, and predictive regularity that stable observers require.

The hypothesis is therefore: the wave-like behaviour of the microcosm is not a primitive feature of reality but the signature of compressed information as perceived from within. An observer composed of compressed structures will perceive their world as wave-governed for the same reason that a pixel-observer would perceive DCT dynamics: the compression codec *is* the physics.

2.2 The Dithering Analogy and the Born Rule

The Born rule — the identification of measurement probabilities with squared wavefunction amplitudes — has a natural interpretation under this hypothesis.

Consider a rendering engine producing a sphere with intended shading intensity 0.85, on hardware restricted to discrete outputs of 0.8 or 0.9. The engine employs *dithering*: distributing 0.8 and 0.9 across adjacent pixels with relative frequencies 0.15 and 0.85 respectively, so that the perceived average matches the target. The discrete output statistics are determined by the continuous target value.

A quantum superposition

$$|\psi\rangle = \alpha|0.8\rangle + \beta|0.9\rangle$$

is the universe's implementation of this same principle. The Born rule $P = |\alpha|^2$ is the probability rule of an optimally compressed continuous description rendered through a discrete measurement apparatus. The squaring arises because amplitudes are complex-valued: the information-theoretic weight of a mode is proportional to the power in that mode, which is the squared amplitude.

This does not constitute a derivation of the Born rule — that would require a proof from the spectral complexity axioms alone. It is offered as a motivation: the Born rule is what optimal compression looks like when a continuous description meets a discrete measurement.

3 Spectral Complexity

3.1 From Kolmogorov to Spectral Complexity

Kolmogorov complexity provides the theoretical foundation for minimal description length but is fundamentally uncomputable, discrete, and discontinuous. It cannot smoothly support stable prediction, continuous spacetime geometry, or the gradual evolutionary reasoning of an internal observer.

The observational evidence suggests that physical systems already possess a natural mode of information representation: decomposition into spectral modes. This motivates a continuous, computable replacement.

Definition 1 (Spectral Complexity)**.** The *spectral complexity* $C_s(\Psi)$ of a state Ψ is the total informational cost required to uniquely specify the amplitudes, frequencies, and phases of the spectral modes composing Ψ:

$$C_s(\Psi) = C_{\text{base}} + \sum_{i=1}^{N} \left[C(\phi_i) + C(A_i) + \frac{\omega_i}{\Delta\omega} \right]$$

where C_{base} is the $\mathcal{O}(1)$ cost of the underlying trigonometric subroutines, $C(\phi_i)$ is the fixed-width bit cost of encoding the phase $\phi_i \in [0, 2\pi)$, $C(A_i)$ is the bit depth required to encode amplitude A_i, and $\omega_i/\Delta\omega$ is the dominant term representing the linear resource cost of tracking mode frequency ω_i relative to the minimum resolution $\Delta\omega$.

Three properties of this measure are essential.

Computability. Unlike Kolmogorov complexity, C_s is directly computable from the spectral decomposition of any state.

Continuity. C_s assigns a smooth, continuous cost gradient across neighbouring states. Small perturbations in frequency or amplitude produce small changes in complexity.

Linear frequency scaling. The dominant cost term $\omega_i/\Delta\omega$ scales linearly with frequency. This mirrors the physical relation $E = \hbar\omega$: energy scales linearly with frequency. Under Solomonoff suppression $P \propto 2^{-C_s}$, this linear cost produces exponential suppression of high-frequency modes:

$$P \propto 2^{-\omega/\Delta\omega} = e^{-(\ln 2)\,\omega/\Delta\omega},$$

which is a Boltzmann distribution with $\beta = \ln 2/\Delta\omega$. The identification $\hbar = \Delta\omega/\ln 2$ connects the minimum frequency resolution of the spectral complexity measure to Planck's constant. This is not a derivation but a precise identification that warrants further investigation.

3.2 Resolution of the Boltzmann Brain Problem

Under the Solomonoff prior $P(s) \propto 2^{-L(s)}$ applied to spectral complexity, the probability of a configuration is exponentially suppressed by its spectral cost. Chaotic, high-entropy configurations — Boltzmann brains, random fluctuations, disordered universes — have high spectral complexity: they require many high-frequency modes with large amplitudes to describe. Their probability under C_s is therefore exponentially suppressed relative to smooth, law-like, compressible configurations.

This resolves the Boltzmann brain problem without additional axioms. The selection of structured observers is not a fine-tuning accident. It is a direct consequence of the measure: smooth, predictable data compresses better than chaos, and the spectral complexity measure weights configurations by their compressibility. We do not find ourselves in a chaotic universe because chaotic universes are exponentially expensive to describe.

4 Numerical Results

4.1 Emergence of Smooth Spacetime

Applying the spectral complexity cost function as a selection weight to the bitstring evolution of Paper II — replacing uniform sampling with C_s-weighted sampling — immediately suppresses the high-entropy white noise of the unweighted ensemble. The dominant configurations are those with low spectral complexity: smoothly varying, wave-governed spatial profiles. Symmetric wave packets and lattice-like structures emerge as the most probable outcomes without being hard-coded.

4.2 Emergence of Inertia and Interference

Two specifically quantum-mechanical phenomena emerge from spectral compression in numerical simulation, without any imposed equations of motion.

Inertia. A localised wave packet moving through the spectral field maintains its velocity without external forcing. The minimum-C_s continuation of a moving packet is the packet continuing to move: any deflection increases the spectral cost by introducing new frequency components. Resistance to deflection — inertia — is the geometric consequence of spectral economy.

Interference. When two wave packets overlap, the minimum-C_s description of the combined state is not the sum of two independent descriptions but a single spectral decomposition of the superposition. The cross-terms — interference fringes — are cheaper to encode than two separate packets

because they share spectral modes. Interference emerges as the compression-optimal description of overlapping structures.

Simulation videos demonstrating both phenomena are available at https://github.com/juhameskanen/abstract/blob/main/gallery/emergent_gravity.gif.

5 The Central Conjecture: $C_s \propto S_{\text{Euclidean}}$

5.1 Background

Hawking's Euclidean path integral approach to quantum gravity [2] computes the wave function of the universe by summing over all compact Euclidean geometries weighted by e^{-S_E}, where S_E is the Euclidean action obtained by Wick rotation $t \to -i\tau$. The minimum-action path through configuration space corresponds to the most probable geometry — the classical solution — while quantum corrections arise from fluctuations around it.

The Wheeler–DeWitt equation [1]

$$\hat{H}|\Psi\rangle = 0$$

expresses the same content in canonical form: the universe has no external time, consistent with the static, timeless axiom of Paper I. The wavefunction of the universe is a solution to this constraint.

5.2 Numerical Path Comparison

We implemented both the minimum-C_s path and the minimum-Euclidean-action path on a 256×256 surface containing two Gaussian potential peaks (Figure 1, left panel). The minimum-C_s path was computed by selecting, at each step, the continuation that minimises the spectral complexity increment. The minimum Euclidean action path was computed by standard variational methods.

Figure 1 (right panel) shows the two paths plotted as amplitude versus position along the x-axis. The Euclidean action path (red) and the informational action path (blue dashed) track each other closely across the full trajectory, including the sharp minimum near $x = 8$ where the path descends between the two potential peaks. The agreement is qualitative but robust: both paths select the same geometric route through the potential landscape.

5.3 The Conjecture

The numerical correspondence motivates the following:
Conjecture 1 (Informational Action Principle)**.** Let Ψ be a path through the configuration space of a finite informational system with bit count n. Let $C_s(\Psi)$ denote the spectral complexity of Ψ and $S_E(\Psi)$ denote the Euclidean action of the corresponding geometric path. Then:

$$C_s(\Psi) \propto S_E(\Psi),$$

with proportionality constant determined by n and the minimum frequency resolution $\Delta\omega$.

If Conjecture 1 holds, the consequences are immediate:

- The Euclidean path integral $\int \mathcal{D}g\, e^{-S_E}$ is the Solomonoff prior $\sum_\Psi 2^{-C_s(\Psi)}$ over spectral configurations. Quantum gravity is Solomonoff induction over compressed descriptions of geometry.

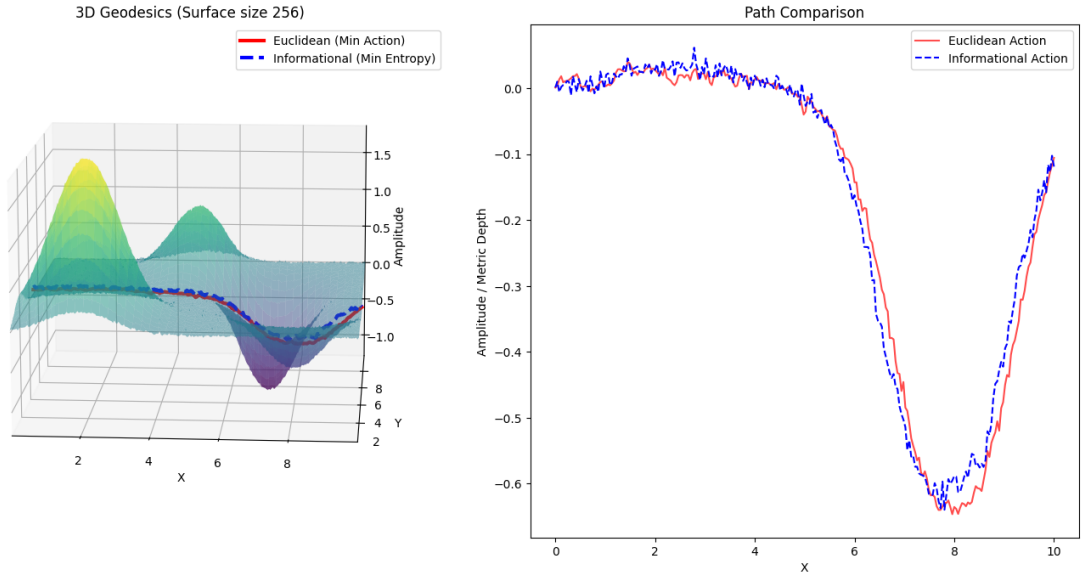

Figure 1: Left: 3D potential surface (256×256) with two Gaussian peaks. The red curve shows the minimum Euclidean action path; the blue dashed curve shows the minimum spectral complexity (informational action) path. Right: Path comparison projected onto the x-axis. Euclidean action (red solid) and informational action (blue dashed) track each other closely across the full trajectory, including the deep minimum near $x = 8$. The correspondence is numerical and qualitative; a rigorous proof of proportionality is the primary open problem of this paper.

- The Wheeler–DeWitt constraint $\hat{H}|\Psi\rangle = 0$ expresses the timelessness of Paper I: the universe has no external clock, and the wavefunction is the spectral complexity distribution over all configurations consistent with the bit budget n.
- The Planck constant $\hbar$ is identified with $\Delta\omega / \ln 2$: the minimum spectral resolution of the informational system, converted from nats to bits.

6 Discussion

6.1 What Has Been Established and What Has Not

This paper establishes the following. The WCP hypothesis is internally consistent with the framework of Papers I–V and resolves the Boltzmann brain problem without new axioms. Spectral complexity is a well-defined, continuous, computable measure that suppresses chaotic configurations exponentially. Inertia and interference emerge numerically from spectral compression without imposed dynamics. The minimum-C_s path and the minimum Euclidean action path agree numerically on a test surface.

This paper does not establish the following. The Born rule is not derived from spectral complexity axioms. The conjecture $C_s \propto S_E$ is not proved. The identification $\hbar = \Delta\omega / \ln 2$ is a correspondence, not a derivation. These are the primary targets for subsequent work.

6.2 Relation to Existing Approaches

Verlinde's entropic gravity [8] derives Newtonian gravity from thermodynamic entropy gradients. Jacobson [3] derives the Einstein field equations from the thermodynamics of local Rindler horizons. Both approaches recover gravitational dynamics from information-theoretic principles. The present framework is complementary: rather than deriving gravitational equations from entropy, it proposes that the path-integral measure of quantum gravity is the spectral complexity prior, and that the two are proportional.

6.3 The Role of n

Throughout Papers I–VI, the integer n plays the role of the universe's single free parameter. Paper IV showed that $n \approx 184$ bits, calibrated against the inflationary aspect ratio. The proportionality constant in Conjecture 1 is expected to depend on n and $\Delta\omega$. A complete theory would express both $\hbar$ and G as functions of n alone, eliminating all free parameters from fundamental physics.

7 Conclusion

This paper establishes three results and states one conjecture.

First, the Wavefunction Compression Principle provides a hypothesis for why the microcosm waves: internal observers composed of compressed structures perceive their world as wave-governed because the compression codec of the universe is the wavefunction. This hypothesis is consistent with all results of Papers I–V and requires no new axioms.

Second, spectral complexity — a continuous, computable replacement for Kolmogorov complexity with linear frequency cost — exponentially suppresses chaotic configurations under Solomonoff-like induction. Structured, law-like, compressible universes dominate the measure. The Boltzmann brain problem is resolved as a consequence of the measure, not by fine-tuning.

Third, numerical simulation demonstrates that inertia and interference emerge from spectral compression alone, without imposed equations of motion, and that the minimum spectral complexity path through a potential landscape agrees numerically with the minimum Euclidean action path.

Conjecture (Informational Action Principle): $C_s \propto S_{\text{Euclidean}}$, with proportionality constant determined by n and $\Delta\omega$. If proved analytically or demonstrated to arbitrary numerical precision, this conjecture identifies quantum gravity as Solomonoff induction over compressed geometric descriptions, completes the bridge from the informational framework of Papers I–VI to a full theory of quantum gravity, and derives $\hbar$ as the minimum spectral resolution of a finite informational universe.

Open Problems

1. **Prove Conjecture 1.** Either analytically, by showing that the spectral complexity functional and the Euclidean action functional are proportional under the informational metric of Paper IV; or numerically, by extending the path comparison to higher-dimensional surfaces and quantifying the deviation.
2. **Derive the Born rule.** Show that $P = |\alpha|^2$ follows from the spectral complexity axioms, using Gleason's theorem or a direct information-theoretic argument.

3. **Derive $\hbar$ from n.** If $\hbar = \Delta\omega / \ln 2$ and $\Delta\omega$ is the minimum frequency resolution of a system with n bits, express $\hbar$ as a function of n and verify against the observed value using $n \approx 184$ from Paper IV.

4. **Derive G from n.** Paper IV recovered Bekenstein–Hawking entropy up to 4π without using G. A complete theory should express Newton's constant as a function of n alone.

Simulation Code

- Spectral compression POC, emergent inertia and interference: https://github.com/juhameskanen/abstract
- Path comparison (minimum C_s vs minimum Euclidean action): supplementary material `simulations/path_comparison.py`

References

[1] Bryce S. DeWitt. "Quantum Theory of Gravity. I. The Canonical Theory". In: *Physical Review* 160.5 (1967), pp. 1113–1148.

[2] Stephen W. Hawking. "The path-integral approach to quantum gravity". In: *General Relativity: An Einstein Centenary Survey*. Ed. by Stephen W. Hawking and Werner Israel. Cambridge: Cambridge University Press, 1979, pp. 746–789.

[3] Ted Jacobson. "Thermodynamics of Spacetime: The Einstein Equation of State". In: *Physical Review Letters* 75.7 (Aug. 1995), pp. 1260–1263. DOI: 10.1103/PhysRevLett.75.1260.

[4] Juha Meskanen. "Black Hole Singularities as Zero-Entropy States". In: *Unpublished Manuscript* (2002).

[5] Juha Meskanen. "Emergent Spacetime Structures from Zero-Entropy Initial States". In: *Unpublished Manuscript* (2003).

[6] Juha Meskanen. "The Axiomatic Foundations of Reality". In: *Unpublished Manuscript* (2001).

[7] Juha Meskanen. "The Geometry of Spacetime as an Information-Theoretic Structure". In: *Unpublished Manuscript* (2026).

[8] Erik Verlinde. "On the origin of gravity and the laws of Newton". In: *Journal of High Energy Physics* 2011.4 (2011), p. 29.